Journal of Thermal Engineering
Web page info: https://jten.yildiz.edu.tr
DOI: 10.14744/jten.2021.0005

Research Article

Flow behavior and thermal separation mechanism on vortex tube

Dedy zulhidayat NOOR[1]*, Heru MIRMANTO[1], Joko SARSETIYANTO[1], Denny M.E.SOEDJONO[1]

[1]Department of Industrial Mechanical Engineering,
Sepuluh Nopember Institute of Technology, Surabaya, Indonesia

ARTICLE INFO

Article history
Received: 02 July 2019
Accepted: 08 October 2019

Key words:
Vortex tube; Flow field;
Thermal separation;
Numerical study

ABSTRACT

Flow behaviour and thermal separation mechanism on vortex tubes have been studied numerically. Rapid expansion indicated by high-pressure gradient near the inlet and the exit ports contributes to energy separation on the parallel and the counter flow vortex tubes. It creates a cooling process at the core region and drives an internal and rotational energy transfer to the peripheral region, then increases the gas temperature at the periphery along with friction due to the presence of the confined wall. Static temperature is related to static pressure in such a way that low pressure leads to the low static temperature at the same region inside the vortex tube. On the other hand, the high total temperature is found in the region with the low dynamic velocity. For both vortex tubes, the flow fields are mainly governed by the tangential velocity at the periphery and by the axial velocity at the core region. The maximum Mach number values based on the maximum tangential velocities in the inlet area for the counter and the parallel flow vortex tubes are 0.689 and 0.726, respectively, so both are compressible and subsonic flows. For the same size of geometry and boundary conditions, the parallel flow vortex tube has higher COP than the counter flow vortex tube i.e. 0.26 and 0.25, respectively.

Cite this article as: Noor DZ, Mirmanto H, Sarsetiyanto J, Soedjono DME. Flow behavior and thermal separation mechanism on vortex tube. J Ther Eng 2021;7(5):1090–1099.

INTRODUCTION

A vortex tube is a thermal-mechanical device that splits an inlet compressed gas into two streams at the outlet with higher and lower temperatures than the inlet one. It has no moving parts, electrical and chemical processes involved which make its maintenance is free, simple operation and durable, furthermore allowed the use of vortex tube in many engineering applications. The thermal separation phenomena in the vortex tube werefirstly introduced by Ranque [1]. More detailed experimental work then carried out by Hilsch [2] to confirm this phenomenon and then it is well-known as Ranque-Hilsch Vortex Tube (RHVT).

***Corresponding author.**
*E-mail address: zulnoor@me.its.ac.id

This paper was recommended for publication in revised form by Regional Editor Jovana Radulovic

Published by Yıldız Technical University Press, İstanbul, Turkey

Since its invention, many works have been performing to explain a thermal separation mechanism on RHVT. Deissler and Perlmutter [3] analysed the flow and energy separation in a turbulent vortex. They stated that the thermal separation took place only if the fluid is compressible and was influenced by the tangential velocity profile. The turbulent shear work done on the fluid element affected the total temperature change significantly. The fluid in the core region offered shear work on the fluid in the outer region with a resultant total temperature separation. Linderstrim-Lang [4] performed experimental work to study gas separation in the Ranque-Hilsch Vortex tube. The sign of separation effect depended on hot flow fraction, ratio tube diameter to two orifices and inlet diameter to tube length. Takahama and Kawamura [5] investigated performance characteristics of energy separation in a stream-operated vortex tube experimentally. The same energy separation performance with air was expressed as far as steam was in the superheated region at the nozzle outlet. When steam was in the wet region at the nozzle outlet, even though steam supplied wassuperheated, the performance considerably decreased due to the energy waste from moisture evaporation and there was no effective energy separation when the dryness fraction at the nozzle outlet was less than 0.98. Through analysis and experiment, Kurosaka [6] attempted to explain that the acoustic streaming induced by orderly disturbances within the swirling flow is the main cause of the Ranque-Hilsch effect in whichenergyis transferredfrom the cold-core to the hot peripheral region. Based on the experiment results, Ahlborn and Groves [7] showed the existence of a secondary circulation in the vortex tube which can be considered as the operating fluid in a classic thermodynamic refrigerant cycle.

By following the rapid development of computing technology, computational fluid dynamics (CFD) is undergoing significant expansion and become a sophisticated and powerful analysis technique thatencompasses a wide range of fluid-thermal problems. Some recent works have utilized CFD modelling to study flow behaviour and energy separation produced by vortextubes. Flohlingsdorf and Unger [8] performed numerical investigations of the compressible flow and the energy separation in Ranque–Hilsch vortex tube using CFX code with *k-ε* turbulent model. Farouk and Farouk [9] carried out large-eddy simulations of the flow field and temperature separation in the Ranque–Hilsch vortex tube.Simulations were conducted for different cold mass fractionsby changing the hot end pressure. The hot exit temperature separation was observed to increase with an increase in the cold mass fraction. Bahera et al. [10] have done numerical investigations on flow behaviour and energy separation in Ranque–Hilsch vortex tube. Investigations have been done on the variation of fluid properties and flow parameters as the fluid particles progress in the flow field by tracking different particles exiting through the hot and cold end. Baghdad et al. [11] conducted a numerical study of energy separation in a vortex tube with different turbulence models, namely, standard *k*-ε, *k*-ε, SST *k*-ω, and RSM models. Four cases with different inlet pressure have been considered. All the applied models were observed to be capable of predicting fairly well the general flow features.

Pouriya et al. [12] have investigated the thermal separation flow characteristic in a vortex tube using a three-equation turbulence model. They concluded that the energy separation, cold-end side temperature and rise in temperature in the peripheral region depend mainly on the ratio of cold and hot-end side mass flow rates, the inlet conditions and swirling flow with high order tangential velocity.

Hamdan et al. [13] performed experimental work to study energy separation inside vortextube for different tube designs. Different tube lengths, diameters, internal tapering angles and, inlet pressure were parameters used in the experiment. A tapering angle smaller than 4° and higher inlet pressure created a greater temperature difference between the hot and cold end.

More recently, Guo et al. [14] have made a critical review of the flow structure studies of Ranque–Hilsch vortex tubes. Earlier methods can only provide qualitative results until newer methods with quantitative results such as numerical methods have been reviewed. Although not very clear yet, several advances in information regarding the relationship between flow structure and energy separation have been achieved. Finally, they concluded that more elaborate and convincing experiments and modelling still need to be established to reveal the energy separation phenomena in a vortex tube.

Most of the studies regarding RHVT including the above-mentioned literature were focused on counter flow vortex tubes. There is limited information about the parallel flow vortex tube. There are three aims for this work. Firstly, this work intends to provide numerical simulations for both counter and parallel flow vortex tubes. Secondly, the flow field and thermal characteristics, as well as energy separation, are discussed. Thirdly, some similarities and differences between the two vortex tube models regarding flow structures and performances are underlined.

THE GOVERNING EQUATIONS

3D flow inside the vortextube is defined as compressible and turbulent with a high rotating condition. Steady-state is assumed and the standard k-ε is applied for the turbulent model. This turbulent model had been used by Bramo et al. [15] and Pourmahmoud et al. [16] and had a good agreement with the experimental data. Furthermore, the same model is used in this work, the governing equations are arranged by the conservation of mass, momentum and energy equations as follows,

$$\frac{\partial}{\partial x_j}(\rho u_j) = 0 \tag{1}$$

$$\frac{\partial}{\partial x_j}(\rho u_i u_j) = -\frac{\partial p}{\partial x_i} + \frac{\partial}{\partial x_j}\left[\mu\left(\frac{\partial u_i}{\partial x_j} + \frac{\partial u_j}{\partial x_i} - \frac{2}{3}\delta_{ij}\frac{\partial u_k}{\partial x_k}\right)\right] + \frac{\partial}{\partial x_j}\left(-\rho\overline{u_i' u_j'}\right) \quad (2)$$

$$\frac{\partial}{x_i}\left[u_i\rho\left(h + \frac{1}{2}u_j u_j\right)\right] = \frac{\partial}{\partial x_j}\left[k_{eff}\frac{\partial T}{\partial x_j} + u_i(\tau_{ij})_{eff}\right], \quad k_{eff} = K + \frac{c_p\mu_t}{\mathrm{Pr}_t} \quad (3)$$

The turbulence kinetic energy (k) and the rate of dissipation (ε) are derived from the equations:

$$\frac{\partial}{\partial t}(\rho k) + \frac{\partial}{\partial x_i}(\rho k u_i) = \frac{\partial}{\partial x_j}\left[\left(\mu + \frac{\mu_t}{\sigma_k}\right)\frac{\partial k}{\partial x_j}\right] + G_k + G_b + \rho\varepsilon - Y_M \quad (4)$$

$$\frac{\partial}{\partial t}(\rho\varepsilon) + \frac{\partial}{\partial x_i}(\rho\varepsilon u_i) = \frac{\partial}{\partial x_j}\left[\left(\mu + \frac{\mu_t}{\sigma_\varepsilon}\right)\frac{\partial \varepsilon}{\partial x_j}\right] + C_{1\varepsilon}\frac{\varepsilon}{k}(G_k + C_{3\varepsilon} + G_b) - C_{2\varepsilon}\rho\frac{\varepsilon^2}{k} \quad (5)$$

The turbulent viscosity, μ_t, is defined by:

$$\mu_t = \rho C_\mu \frac{k^2}{\varepsilon} \quad (6)$$

G_k and G_b reveal the generation of turbulent kinetic energy due to the mean velocity gradient and buoyancy, respectively, while Y_M represents the contribution of the fluctuating dilation on compressible turbulence to the overall dissipation rate.σ_k and σε are the turbulent Prandtl numbers (Pr) of k and ε, respectively. $C\mu$, $C_{1\varepsilon}$ and, $C_{2\varepsilon}$ are constants. Our study does not focus on variations in the value of these constants to their effects on simulation results. The model constants $C_{1\varepsilon}$, $C_{2\varepsilon}$, C_μ, σ_k and σ_ε have the following default values in Ansys-fluent i.e. $C_{1\varepsilon} = 1.44$, $C_{2\varepsilon} = 1.92$, $C_\mu = 0.09$, $\sigma_k = 1.0$, and $\sigma_\varepsilon = 1.3$.

The energy conservation condition related to the total temperature inside a vortex tube is defined by

$$T - \frac{\bar{v}\cdot\bar{\omega}\times\bar{r}}{c_p} = const \quad (7)$$

where T is the total or stagnation temperature of the rotating gas at the radial position while v, ω and c_p are the absolute gas velocity as observed from the stationary frame of reference, the angular velocity of the system and the isobaric heat capacity of the gas, respectively.

Model Description

The two models are described in Figure 1. The diameter of the vortex tube is 1 cm with aworking length of 10 cm. The diameter and length of the cold port are 0.3 cm and 0.5 cm, respectively. The hot exit is an annulus with an area of 0.14815 cm^2. There are four square inlet ports. Each inlet port has an area of 0.2 × 0.2 cm^2. Air is chosen as working fluid with the inlet pressure 5 bar while the atmospheric condition is used at the exit.

Numerical Validation

This article is purely a numerical method and the chosen model has no resemblance to any experimental model in previous studies. The numerical method used in this work is validated with the experimental and numerical works of [17]. The validated model is shown in Figure 2 and the static gauge pressure at the outlet is shown in Figure 3.

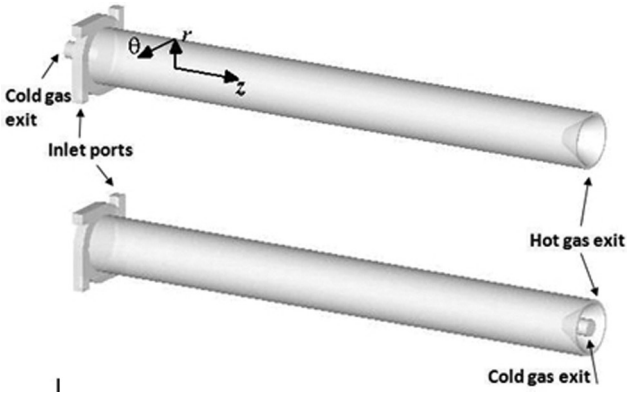

Figure 1. The models for the counter-flow (upper) and the parallel-flow (lower) vortex tubes.

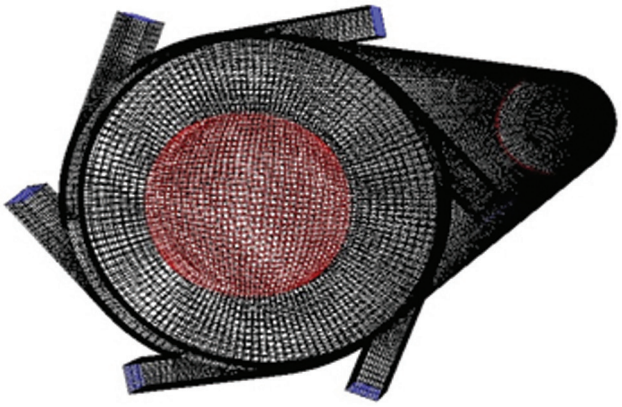

Figure 2. Validated model.

From Figure 3 it appears that the 2D CFD model got over-prediction results compared to the experimental results, whereas the present 3D model has under-predictions than the experiments. Qualitatively there is an agreement between the results of the CFD model with the experiments.

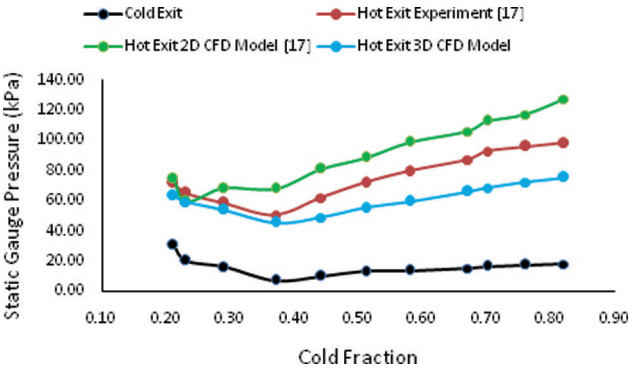

Figure 3. The hot and cold exit static pressure as a function of the cold fraction.

For our works, the chosen model of the parallel-flow vortex tube is the same as the previous study [18] and it has a grid independence study with a 500,335 grid numbers. Then we use the same dimensions and number of grids for the counter-flow vortex tube (Figure 1).

From Figure 3 it appears that the 2D CFD model got over-prediction results compared to the experimental results, whereas the present 3D model has under-predictions than the experiments. Qualitatively there is an agreement between the results of the CFD model with the experiments.

For our works, the chosen model of the parallel-flow vortex tube is the same as the previous study [18] and it has a grid independence study with 500,335 grid number. Then we use the same dimensions and number of grids for the counter-flow vortex tube (Figure 1).

RESULTS AND DISCUSSION

The flow field inside the vortex tube is mainly governed by tangential, angular and axial velocities. Figures 4, 5 and

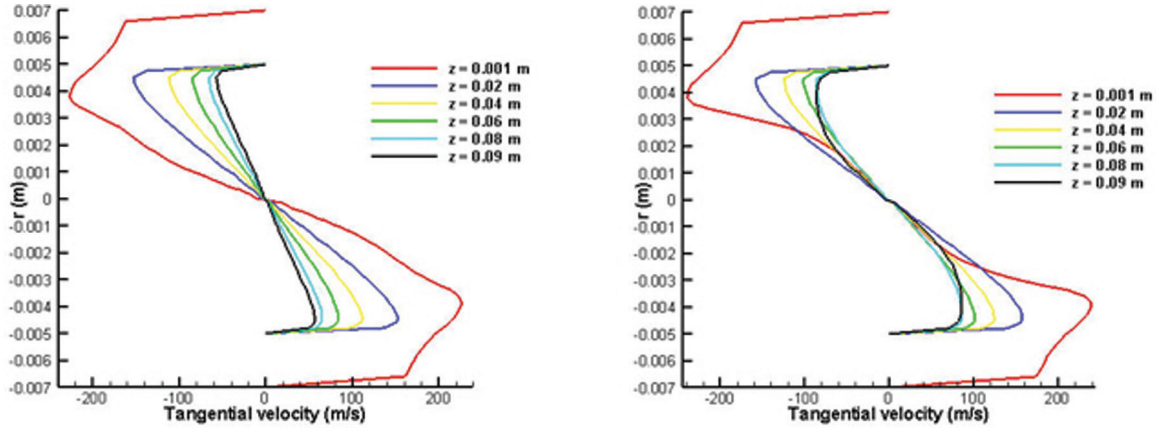

Figure 4. Tangential velocity profile,the counter flow (left) the parallel flow (right).

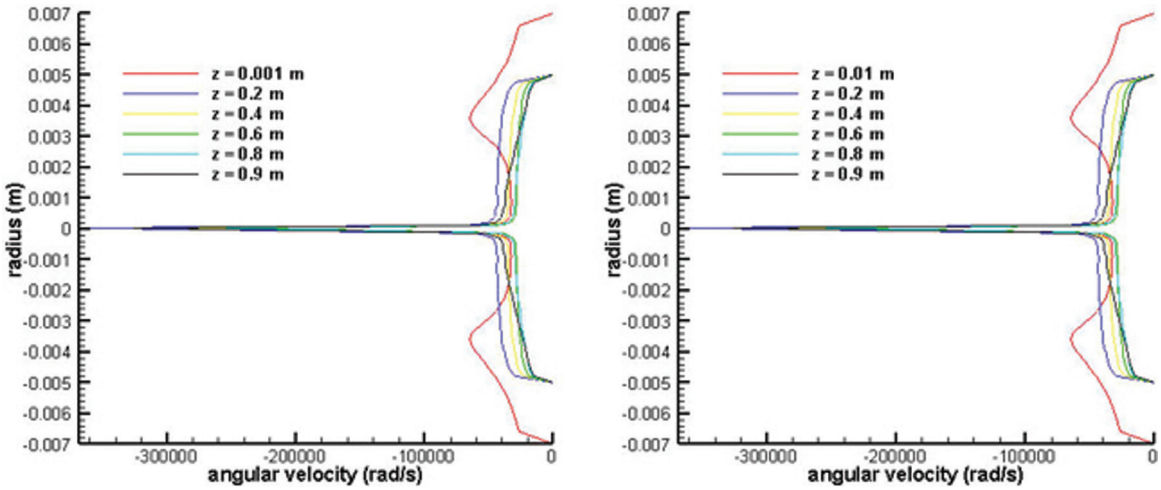

Figure 5. Angular velocity for the counter (left) and the parallel (right) flow vortex tube.

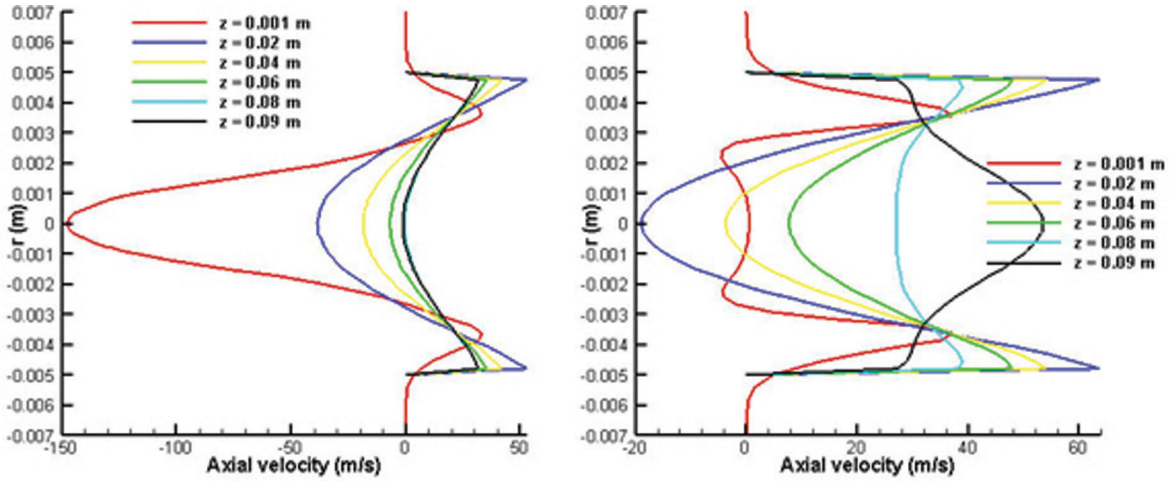

Figure 6. Axial velocity profile for **a.** the counter (**left**) and **b.** the **parallel** (**right**) flow vortex tube.

6 show these velocity components. The tangential velocity profile along z (axial) direction is identic for counter flow and parallel flow vortex tubes. The tangential/swirl velocity has the maximum magnitude near the nozzle inlet as the result of a tangential injection of air. The highest tangential velocities are found at positions $r = 0.004\ mm$ and $z = 0.001\ m$ in both counter and parallel flow with values of 229 ms^{-1} and 240 ms^{-1} respectively. Based on the velocities and temperature data, the maximum Mach number values for the counter and parallel flow vortex tubes are 0.689 and 0.726, respectively. Both are compressible flow but still in the subsonic flow regime. This tangential velocity decreases as the fluid progress along the axial direction and the minimum magnitude is found near the hot gas exit ($z = 0.09\ m$). Different from the inlet, in this exit area, the maximum tangential velocity is found at $r = 0.0045\ m$ which is equal to 59 ms^{-1} for counter flow and 86 ms^{-1} for parallel flow.

Tangential velocity is related to the distance r from the axis of rotation. The swirl flow at the core region is known as forced vortex flow while the peripheral one is defined as free vortex flow as shown in Figure 4. However, a forced vortex in the core near the inlet is found to be the dominating flow structure in the tube. The tangential velocity magnitude is observed to be minimum and even negligible near the tube axis and it increases in the radial direction. The velocity magnitude then decreases after reaching the boundary layer region near the tube wall and finally has the same zero value with the velocity at the core due to the non-slip condition on the wall. Even though the tangential velocity is low at the core region due to its small radius, the angular velocity is found to be higher than the peripheral as shown in Figure 5.

Differ from the tangential velocity, the axial velocity has the highest magnitude at the axis and it is more dominant at the core region than the periphery as shown in Figure 6a. The existence of positive and negative axial velocities shows that air moves to the hot and cold exits at the peripheral

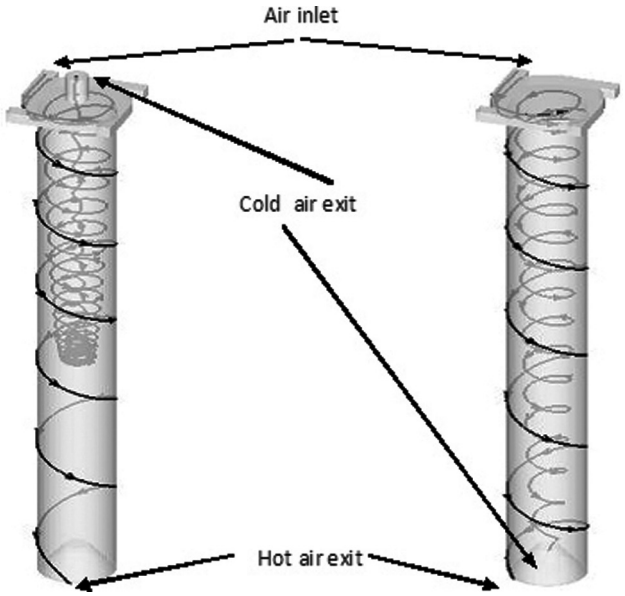

Figure 7. The inner (cold) and the outer (hot) flows.

and core regions, respectively. This velocity decreases when the stream traveling towards a hot exit. The main difference between the counter and parallel flow vortex tube is the axial velocity near the hot exit. For the parallel flow vortex tube, the blockage effect due to a narrow hot exit decelerates the axial velocity at the periphery and deflects some fraction of air flowing towards the cold exit in such a way that the axial velocity at the core (cold exit) has a positive value as shown in Figure 6b for $z = 0.009\ m$. The streamlines plot in Figure 7 has confirmed this condition.

Air expansion occurs in radial and axial directions. This rapid expansion contributes to energy separation in the vortex tube. High static pressure gradients in radial and axial directions are found at the cross-sectional areas near inlet ports ($z = 0.001\ m$ to $z = 0.02\ m$) as shown in Figure 8.

The pressure gradient in the axial direction for counter flow is observed to be higher than parallel flow, especially at the axis near the inlet port. This pressure gradient is found higher in the radial direction than the axial direction. For both vortex tubes, a weakening pressure gradient occurs in the direction offlow. Low static pressure at the core region increases sharply at the beginning then this pressure increase is slowed when air flows toward the exit. On the other hand, for the periphery, high static pressure near the inlet decreases as air moves toward the exit.

The dynamic pressures for both vortex tubes are plotted in Figure 9. It can be observed that the highest dynamic pressure at any section in the axial direction is found at the boundary between the core and peripheral regions. This dynamics pressure is contributed by tangential velocity (Figure 4) and axial velocity (Figure 6). The high dynamic velocity at the peripheral region is caused by the high tangential velocity while the dynamic velocity at the core is mostly contributed by the axial velocity. The total pressure plot in Figure 10 reveals the energy contained by fluid. It has a similar model tothe static pressure plot in Figure 8. The high pressure at inlet flow separates to become the lower pressure at hot and cold exits.

The high-pressure gradient indicates the high energy separation and it can be found near the cold exit. This energy separation diminishes toward the hot exit when

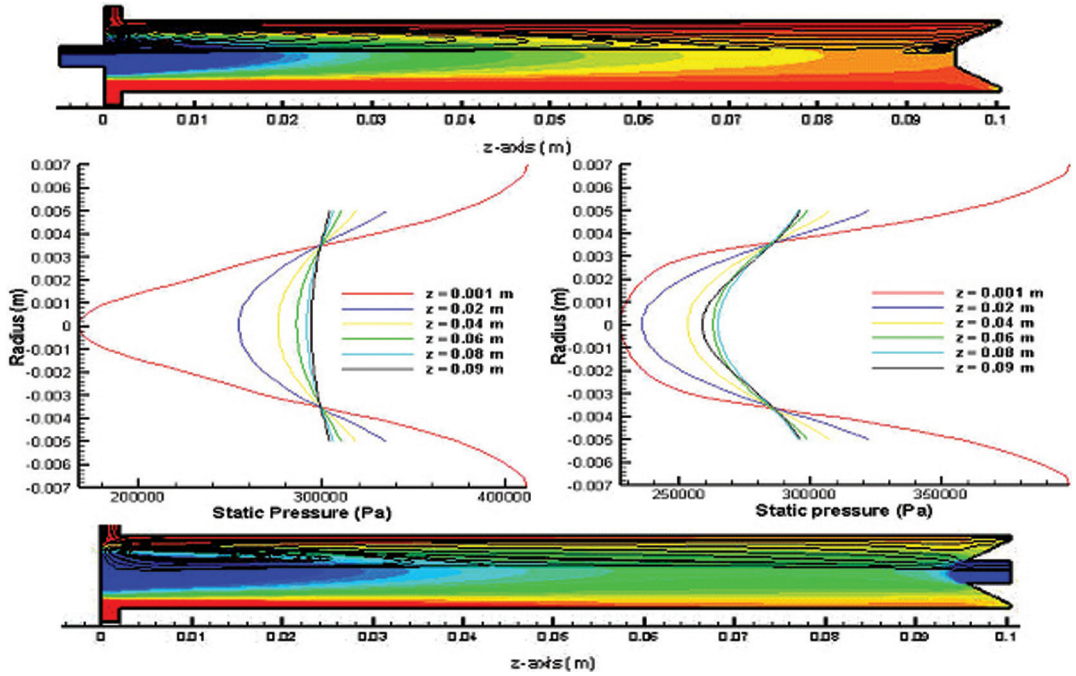

Figure 8. Streamlines and static pressure field for the counter (left-upper) and the parallel (right-lower) vortex flow.

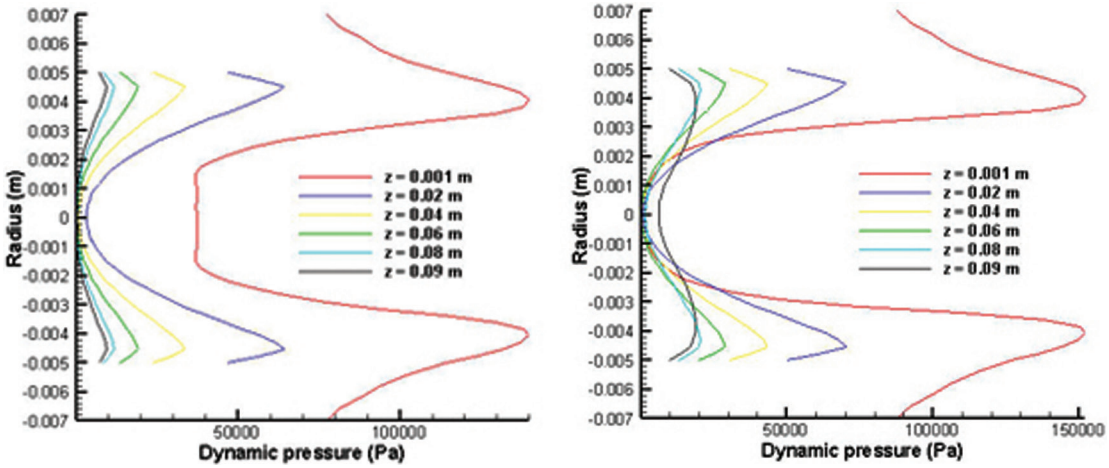

Figure 9. Dynamics pressure for the counter (left) and the parallel (right) flow vortex tubes.

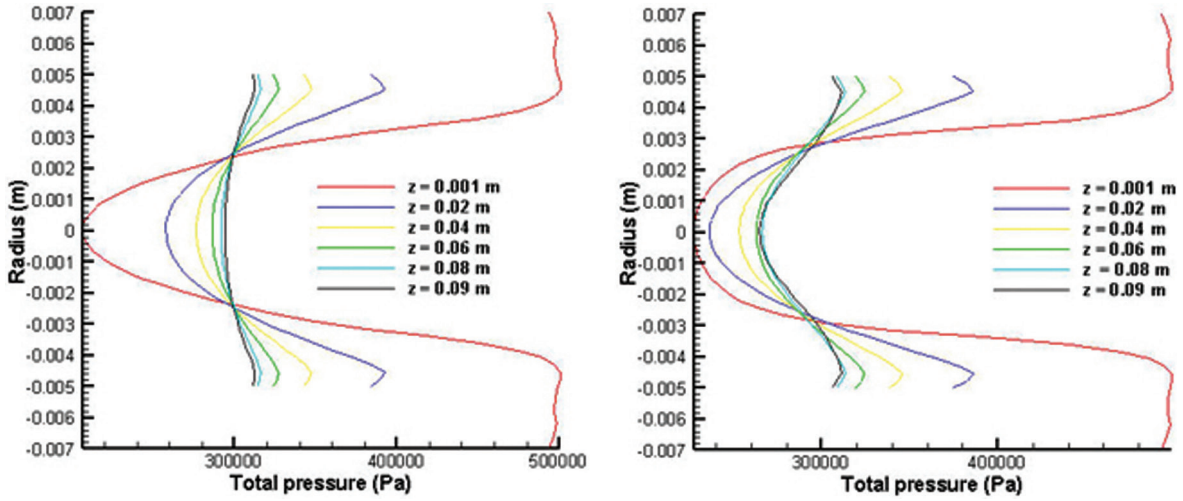

Figure 10. Total pressure plot for the counter (left) and the parallel (right) flow vortex tube.

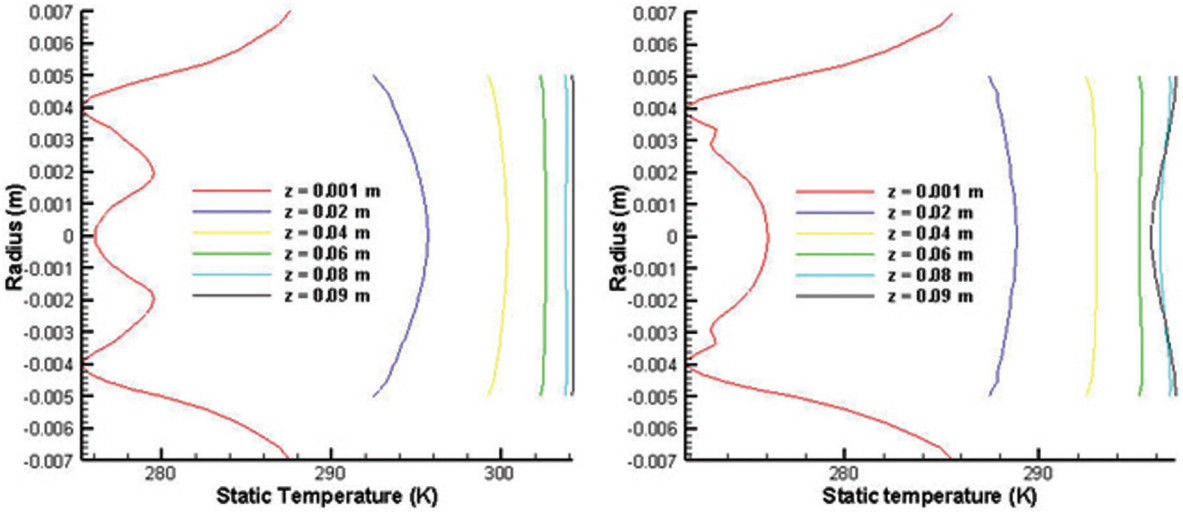

Figure 11. Static temperature plot for the counter (left) and the parallel (right) flow vortex tube.

the radial pressure gradient approaches zero. The static pressure at the exit is related to the static temperature. It is observed that the low static temperature is found in the flow field with low static pressure as shown in Figure 11. The temperature gradients are high in the peripheral and low in the core region. We notify that the static temperature is the measured temperature indicated by a device. On the other hand, the total temperature is related to the dynamic pressure or velocity. The low total temperature is resulted fromhigh dynamic velocity in the flow field. The high tangential and axial velocities near the inlet as indicated in Figure 4 and 6 ($z = 0.001m$) cause the low total temperature in that region (Figure 12). As the flow progress in the axial direction, the velocities decrease and convert to increase the total temperature.

Temperature separation inside a vortex tube can be explained by equation 7 [19]. The equation shows that the gas is getting colder towards the centre of rotation and vice versa. The resulting cooling at the centre of rotation is due to the adiabatic expansion of the gas as well as the conservation of angular momentum. The high angular velocity (Figure 5) demands a transfer of internal and rotational energy to the outer layer of the rotating gas. Since the vortex is confined by the wall, the gas temperature at the periphery increases due to friction and radial momentum transfer from the core region.

To compare these two vortex tubes, we present some parameters in Table 1. The energy separation in the vortex tube creates a cooling capacity, the coefficient of performance (COP) can then be calculated based on the ratio of the cooling capacity to the compression work. COP for the counter-flow and parallel flow vortex tubes are 0.25 and 0.26, respectively. This different COP is resulted fromdifferent cooling capacities. The counter flow has a lower

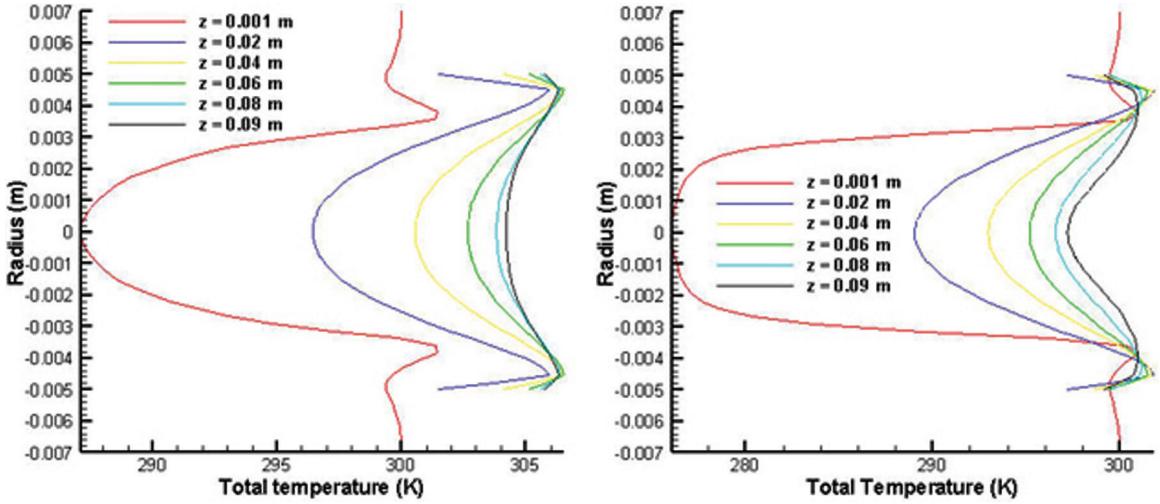

Figure 12. Total temperature plot for the counter (left) and the parallel (right) flow vortex tube.

Table 1. The boundary conditions and the performance parameters

Vortex tube	Inlet pressure P_{in}	Outlet pressure P_{out}	Cold temperature T_{cold}	Cold mass flow rate $\dot{m}_c$	COP	Mach number, M
Counter flow	5 bar	1 bar	247.1 K	0.0042 $\frac{kg}{s}$	0.25	0.689
Parallel flow	5 bar	1 bar	251.9 K	0.00487 $\frac{kg}{s}$	0.26	0.726

cold temperature at the exit than the parallel flow however the parallel flow has a higher cooling capacity due to the higher cold mass flow rate (cold mass fraction) than the counter-flow.

CONCLUSION

Simulations to study flow behaviour and thermal separation mechanism on vortex tubes have been conducted. An adiabatic rapid expansion of the gas as well as conservation of angular momentum create a cooling process at the core region and drive an internal and rotational energy transfer to the peripheral region, then increase the gas temperature at the periphery along with friction due to the presence of the confined wall. The static pressure and the total pressure have a similar modes for each vortex tube. The static pressure at cold and hot exits is related to the static temperature while the total pressure associated with the sum of static pressure to dynamic pressure. The flow field is mainly governed by the tangential velocity at the peripheral region and by axial velocity as well as high order angular velocity at the core region

The maximum Mach number values in the inlet area for counter and parallel flow vortex tubes are 0.689 and 0.726, respectively, so both are compressible and subsonic flows. For the same size of geometry and boundary conditions, the parallel flow vortex tube has higher COP than the counter flow vortex tube i.e. 0.26 and 0.25, respectively.

NOMENCLATURE

C_p	Specific heat, *kJ / kg K*
COP	Coefficient of performance
k	Turbulence kinetic energy, m^2/s^2
K	Thermal conductivity, W/mK
M	Mach number
P	Pressure, N/m^2
R	Radial direction
T	Temperature, K
u'	Fluctuating component of velocity, m/s
V	Velocity, m/s
z	axial direction
Greek symbols	
ε	Turbulence dissipation rate, m^2/s^3
θ	Tangential direction
ρ	Density of a fluid,
ω	Angular velocity, $1/s$
σ	Stress, N/m^2

μ′	Dynamic viscosity, *kg/m s*
μt′	Turbulent viscosity, *kg/m s*
τ′	Shear stress, N/m^2
τ_{ij}	Stress tensor components

Subscripts

in	Refers to inlet
out	Refers to outlet
c	Refers to cold fluid
h	Refers to hot fluid

DATA AVAILABILITY STATEMENT

No new data were created in this study. The published publication includes all graphics collected or developed during the study.

CONFLICT OF INTEREST

The author declared no potential conflicts of interest with respect to the research, authorship, and/or publication of this article.

ETHICS

There are no ethical issues with the publication of this manuscript.

REFERENCES

[1] Ranque GJ. Experiments on Expansion in a Vortex with Simultaneous Exhaust of Hot and Cold Air. Le Journal De Physique et le Radium 1933; 4: 112–114.

[2] Hilsch R. The Use of the Expansion of Aires in Centrifugal Field as a Cooling Process. Review of Scientific Instrument 1947; 13: 108–113. https://doi.org/10.1063/1.1740893.

[3] Deissler RG, Perlmutter M. Analysis of The Flow and Energy Separation in a Turbulent Vortex. International Journal of Heat and Mass Transfer 1960; 1: 173–191. https://doi.org/10.1016/0017-9310(60)90021-1.

[4] Linderstom-Lang, CU. Gas Separation in The Ranque-Hilsch Vortex Tube, International Journal of Heat and Mass Transfer 1964; 7: 1195–1206. https://doi.org/10.1016/0017-9310(64)90061-4.

[5] Takahama H, Kawamura H. Performance Characteristic of Energy Separation in a Steam-Operated Vortex Tube. International Journal of Engineering Science 1979; 17: 735–744. https://doi.org/10.1016/0020-7225(79)90048-X.

[6] Kurosaka M. Acoustic streaming in swirl flow and the Ranque–Hilsch (vortex-tube) effect. Journal of Fluid Mechanics 1982; 124: 139–172. https://doi.org/10.1017/S0022112082002444.

[7] Ahlborn BK, Groves S. Secondary flow in a vortex tube. Fluid Dyn. Res. 1997; 21: 73–86.

[8] Frohlingsdorf W, Unger H. Numerical investigations of the compressible flow and the energy separation in Ranque–Hilsch vortex tube. International Journal of Heat and Mass Transfer 1999; 42: 415–422. https://doi.org/10.1016/S0017-9310(98)00191-4.

[9] Farouk T, Farouk B. Large eddy simulations of the flow field and temperature separation in the Ranque–Hilsch vortex tube. International Journal of Heat and Mass Transfer 2007; 50: 4724–4735. https://doi.org/10.1016/j.ijheatmasstransfer.2007.03.048.

[10] Behera U, Paul PJ, Dinesh K, Jacob S. Numerical investigations on flow behaviour and energy separation in Ranque–Hilsch vortex tube. International Journal of Heat and Mass Transfer 2008; 51: 6077–6089. https://doi.org/10.1016/j.ijheatmasstransfer.2008.03.029.

[11] Baghdad M, Ouadha A, Imine O, Addad Y. Numerical study of energy separation in a vortex tube with different RANS models. International Journal of Thermal Sciences 2011; 50: 2377–2385. https://doi.org/10.1016/j.ijthermalsci.2011.07.011.

[12] Pouriya HN, Mortaheb HR, Mokhtarani B. Numerical Investigation of a Ranque–Hilsch Vortex Tube Using a Three-Equation Turbulence Model. Chemical Engineering Communications 2016; 204: 327–336. https://doi.org/10.1080/00986445.2016.1155989.

[13] Hamdan MO, Omari SAB, Oweimer AS. Experimental study of vortex tube energy separation under different tube design. Experimental Thermal and Fluid Science 2018; 91: 306–311. https://doi.org/10.1016/j.expthermflusci.2017.10.034.

[14] Xiangji Guo, Bo Zhang, Bo Liu, Xiang Xu. A critical review on the flow structure studies of Ranque–Hilsch vortex tubes. International Journal of Refrigeration 2019; 104: 51–64. https://doi.org/10.1016/j.ijrefrig.2019.04.030.

[15] Bramo AR, Pourmahmoud N. CFD simulation of length to diameter ratio effect on the energy separation in a vortex tube. Thermal Science 2011; 15: 3, 833-848. https://doi.org/10.2298/TSCI101004008B.

[16] Pourmahmoud N, Hassanzadeh A, Moutaby O. Numerical analysis of the effect of helical nozzles gap on the cooling capacity of Ranque-Hilsch vortex tube. International Journal of Refrigeration 2012; 35: 1473–1483. https://doi.org/10.1016/j.ijrefrig.2012.03.019.

[17] Sky HM, Klein SA, Nellis G. Comparison of CFD Analysis to empirical data in a commercial vortex tube. International Journal of Refrigeration 2006; 29: 71–80. https://doi.org/10.1016/j.ijrefrig.2005.05.004.

[18] Noor DZ, Mirmanto H, Sarsetiyanto J, Soedjono DME, Setyawati SB. Numerical study of flow and thermal filed on a parallel flow vortex tube. Engineering 2012; 4: 774–777. doi: 10.4236/eng.2012.411099.

[19] Polihronov JG, Straatman AG. Thermodynamics of angular propulsion in fluids. Physical Review Letters 2012, 109. https://doi.org/10.1103/PhysRevLett.109.054504.